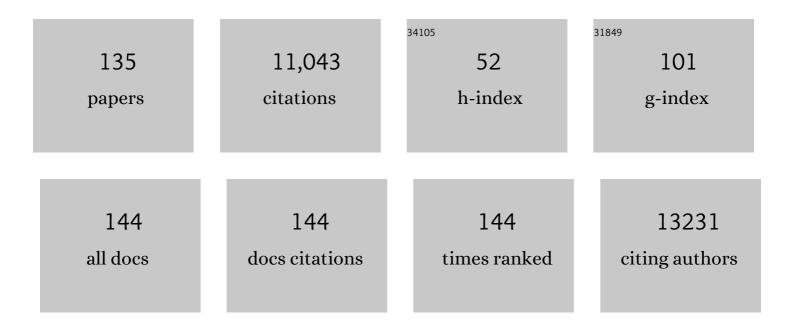
List of Publications by Year in descending order

Source: https://exaly.com/author-pdf/5685968/publications.pdf Version: 2024-02-01



ΙΔΟΠΤ ΝΑΝΙΟΑ

#	Article	IF	CITATIONS
1	Multifunctional Separator Allows Stable Cycling of Potassium Metal Anodes and of Potassium Metal Batteries. Advanced Materials, 2022, 34, e2105855.	21.0	45
2	Nextâ€Generation Cobaltâ€Free Cathodes – A Prospective Solution to the Battery Industry's Cobalt Problem. Advanced Energy Materials, 2022, 12, .	19.5	71
3	Multifunctional Separator Allows Stable Cycling of Potassium Metal Anodes and of Potassium Metal Batteries (Adv. Mater. 7/2022). Advanced Materials, 2022, 34, .	21.0	1
4	Review of modification strategies in emerging inorganic solid-state electrolytes for lithium, sodium, and potassium batteries. Joule, 2022, 6, 543-587.	24.0	90
5	Solid state lithium metal batteries – Issues and challenges at the lithium-solid electrolyte interface. Current Opinion in Solid State and Materials Science, 2022, 26, 100999.	11.5	29
6	Membrane design for non-aqueous redox flow batteries: Current status and path forward. CheM, 2022, 8, 1611-1636.	11.7	16
7	Selective Plasticization of Poly (ethylene oxide) (PEO) Block in Nanostructured Polystyreneâ^' PEOâ^' Polystyrene Triblock Copolymer Electrolytes. Journal of the Electrochemical Society, 2022, 169, 050506.	2.9	1
8	Halide sublattice dynamics drive Li-ion transport in antiperovskites. Journal of Materials Chemistry A, 2022, 10, 15731-15742.	10.3	3
9	Machine Learning Modeling for Accelerated Battery Materials Design in the Small Data Regime. Advanced Energy Materials, 2022, 12, .	19.5	29
10	Modified coal char materials with high rate performance for battery applications. Carbon, 2021, 172, 414-421.	10.3	21
11	Anomalously high elastic modulus of a poly(ethylene oxide)-based composite electrolyte. Energy Storage Materials, 2021, 35, 431-442.	18.0	42
12	Phase evolution during lithium–indium halide superionic conductor dehydration. Journal of Materials Chemistry A, 2021, 9, 990-996.	10.3	19
13	Egyptian blue: from pigment to battery electrodes. RSC Advances, 2021, 11, 19885-19889.	3.6	3
14	Understanding cation-disordered rocksalt oxyfluoride cathodes. Journal of Materials Chemistry A, 2021, 9, 7826-7837.	10.3	21
15	Multifunctional Utilization of Pitchâ€Coated Carbon Fibers in Lithiumâ€Based Rechargeable Batteries. Advanced Energy Materials, 2021, 11, 2100135.	19.5	25
16	High Energy Density and Stable Threeâ€Dimensionally Structured Se‣oaded Bicontinuous Porous Carbon Battery Electrodes. Energy Technology, 2021, 9, 2100175.	3.8	4
17	Robust Solid/Electrolyte Interphase (SEI) Formation on Si Anodes Using Glyme-Based Electrolytes. ACS Energy Letters, 2021, 6, 1684-1693.	17.4	87
18	Molten Salt Assisted Low-Temperature Electro-Catalytic Graphitization of Coal Chars. Journal of the Electrochemical Society, 2021, 168, 046504.	2.9	8

#	Article	IF	CITATIONS
19	Evaluation of electrochemical performance and redox activity of Fe in Ti doped layered P2-Na0.67Mn0.5Fe0.5O2 cathode for sodium ion batteries. Electrochimica Acta, 2021, 380, 138156.	5.2	20
20	Investigating Multiscale Spatial Distribution of Sulfur in a CNT Scaffold and Its Impact on Li–S Cell Performance. Journal of Physical Chemistry C, 2021, 125, 13146-13157.	3.1	24
21	Calibration-Free Quantitative Analysis of Lithium-Ion Battery (LiB) Electrode Materials Using Laser-Induced Breakdown Spectroscopy (LIBS). ACS Applied Energy Materials, 2021, 4, 7259-7267.	5.1	8
22	Toward a mechanically stable solid electrolyte interphase. Matter, 2021, 4, 2119-2122.	10.0	4
23	Anion Coordination Improves High-Temperature Performance and Stability of NaPF6-Based Electrolytes for Supercapacitors. Energies, 2021, 14, 4409.	3.1	4
24	Multifunctional approaches for safe structural batteries. Journal of Energy Storage, 2021, 40, 102747.	8.1	33
25	Formation of LiF Surface Layer During Direct Fluorination of High-Capacity Co-Free Disordered Rocksalt Cathodes. ACS Applied Materials & Interfaces, 2021, 13, 38221-38228.	8.0	13
26	Ambient Temperature Sodium Polysulfide Catholyte for Nonaqueous Redox Flow Batteries. Journal of the Electrochemical Society, 2021, 168, 080540.	2.9	7
27	Heavily Tungstenâ€Doped Sodium Thioantimonate Solid‣tate Electrolytes with Exceptionally Low Activation Energy for Ionic Diffusion. Angewandte Chemie, 2021, 133, 26362-26370.	2.0	2
28	Quantifying the chemical, electrochemical heterogeneity and spatial distribution of (poly) sulfide species using Operando SANS. Energy Storage Materials, 2021, 40, 219-228.	18.0	7
29	Heavily Tungstenâ€Đoped Sodium Thioantimonate Solid‣tate Electrolytes with Exceptionally Low Activation Energy for Ionic Diffusion. Angewandte Chemie - International Edition, 2021, 60, 26158-26166.	13.8	18
30	Challenges and Opportunities for Fast Charging of Solid-State Lithium Metal Batteries. ACS Energy Letters, 2021, 6, 3734-3749.	17.4	76
31	Investigation of glass-ceramic lithium thiophosphate solid electrolytes using NMR and neutron scattering. Materials Today Physics, 2021, 21, 100478.	6.0	5
32	Distilling nanoscale heterogeneity of amorphous silicon using tip-enhanced Raman spectroscopy (TERS) via multiresolution manifold learning. Nature Communications, 2021, 12, 578.	12.8	25
33	Effect of Composition on Mechanical Properties and Conductivity of the Dual-Ion Conductor Na <sub>1+<i>x</i></sub> Mn <sub><i>x</i>/2</sub> Zr <sub>2â€"<i>x</i>/2</sub> (PO <sub>4</sub> ) <sub>3</sub> for Solid-State Batteries. ACS Applied Energy Materials, 2021, 4, 11684-11692.	su <b>b</b> >1	6
34	Separator Effect on Zinc Electrodeposition Behavior and Its Implication for Zinc Battery Lifetime. Nano Letters, 2021, 21, 10446-10452.	9.1	94
35	Dendriteâ€Free Potassium Metal Anodes in a Carbonate Electrolyte. Advanced Materials, 2020, 32, e1906735.	21.0	107
36	Site-Specific Sodiation Mechanisms of Selenium in Microporous Carbon Host. Nano Letters, 2020, 20, 918-928.	9.1	30

#	Article	IF	CITATIONS
37	New synthesis strategies to improve Co-Free LiNi0.5Mn0.5O2 cathodes: Early transition metal d0 dopants and manganese pyrophosphate coating. Journal of Power Sources, 2020, 479, 228591.	7.8	22
38	Lithium Iron Aluminum Nickelate, LiNi <i><sub>x</sub></i> Fe <i><sub>y</sub></i> Al <i><sub>z</sub></i> O <sub>2</sub> —New Sustainable Cathodes for Nextâ€Generation Cobaltâ€Free Liâ€Ion Batteries. Advanced Materials, 2020, 32, e2002960.	21.0	77
39	Direct Measure of Electrode Spatial Heterogeneity: Influence of Processing Conditions on Anode Architecture and Performance. ACS Applied Materials & Interfaces, 2020, 12, 55954-55970.	8.0	21
40	Stable Potassium Metal Anodes with an Allâ€Aluminum Current Collector through Improved Electrolyte Wetting. Advanced Materials, 2020, 32, e2002908.	21.0	70
41	Solvent-Mediated Synthesis of Amorphous Li <sub>3</sub> PS <sub>4</sub> /Polyethylene Oxide Composite Solid Electrolytes with High Li <sup>+</sup> Conductivity. Chemistry of Materials, 2020, 32, 8789-8797.	6.7	21
42	Cathode–Sulfide Solid Electrolyte Interfacial Instability: Challenges and Solutions. Frontiers in Energy Research, 2020, 0, .	2.3	4
43	Investigation of Complex Intermediates in Solvent-Mediated Synthesis of Thiophosphate Solid-State Electrolytes. Journal of Physical Chemistry C, 2020, 124, 27396-27402.	3.1	9
44	Improved Single-Ion Conductivity of Polymer Electrolyte via Accelerated Segmental Dynamics. ACS Applied Energy Materials, 2020, 3, 12540-12548.	5.1	31
45	Hidden Subsurface Reconstruction and Its Atomic Origins in Layered Oxide Cathodes. Microscopy and Microanalysis, 2020, 26, 2542-2544.	0.4	0
46	Nonpassivated Silicon Anode Surface. ACS Applied Materials & amp; Interfaces, 2020, 12, 26593-26600.	8.0	45
47	Synthesizing Highâ€Capacity Oxyfluoride Conversion Anodes by Direct Fluorination of Molybdenum Dioxide (MoO <sub>2</sub> ). ChemSusChem, 2020, 13, 3825-3834.	6.8	12
48	Well-designed Crosslinked Polymer Electrolyte Enables High Ionic Conductivity and Enhanced Salt Solvation. Journal of the Electrochemical Society, 2020, 167, 070539.	2.9	41
49	Operando Acoustic Monitoring of SEI Formation and Long-Term Cycling in NMC/SiGr Composite Pouch Cells. Journal of the Electrochemical Society, 2020, 167, 020517.	2.9	36
50	Potassium Batteries: Dendriteâ€Free Potassium Metal Anodes in a Carbonate Electrolyte (Adv. Mater.) Tj ETQqO	0 0 rgBT /	Ovgrlock 10 1
51	High Capacity Adsorption—Dominated Potassium and Sodium Ion Storage in Activated Crumpled Graphene. Advanced Energy Materials, 2020, 10, 1903280.	19.5	72
52	Hidden Subsurface Reconstruction and Its Atomic Origins in Layered Oxide Cathodes. Nano Letters, 2020, 20, 2756-2762.	9.1	24
53	Multiscale and Multimodal Characterization of 2D Titanium Carbonitride MXene. Advanced Materials Interfaces, 2020, 7, 1902207.	3.7	35

54Elastic Single-Ion Conducting Polymer Electrolytes: Toward a Versatile Approach for Intrinsically<br/>Stretchable Functional Polymers. Macromolecules, 2020, 53, 3591-3601.4.841

#	Article	IF	CITATIONS
55	The influence of FEC on the solvation structure and reduction reaction of LiPF6/EC electrolytes and its implication for solid electrolyte interphase formation. Nano Energy, 2019, 64, 103881.	16.0	239
56	Unraveling the Nanoscale Heterogeneity of Solid Electrolyte Interphase Using Tip-Enhanced Raman Spectroscopy. Joule, 2019, 3, 2001-2019.	24.0	99
57	Interfacial Reactions and Performance of Li <sub>7</sub> La <sub>3</sub> Zr <sub>2</sub> O <sub>12</sub> -Stabilized Li–Sulfur Hybrid Cell. ACS Applied Materials & Interfaces, 2019, 11, 42042-42048.	8.0	34
58	Atomic-Scale Mechanisms of Enhanced Electrochemical Properties of Mo-Doped Co-Free Layered Oxide Cathodes for Lithium-Ion Batteries. ACS Energy Letters, 2019, 4, 2540-2546.	17.4	40
59	Synthesis of metal chloride films: Influence of growth conditions on crystallinity. Thin Solid Films, 2019, 689, 137520.	1.8	3
60	High-Capacity Organic Radical Mediated Phosphorus Anode for Sodium-Based Redox Flow Batteries. ACS Energy Letters, 2019, 4, 2593-2600.	17.4	32
61	A novel P3-type Na <sub>2/3</sub> Mg <sub>1/3</sub> Mn <sub>2/3</sub> O <sub>2</sub> as high capacity sodium-ion cathode using reversible oxygen redox. Journal of Materials Chemistry A, 2019, 7, 1491-1498.	10.3	122
62	Tailored crosslinking of Poly(ethylene oxide) enables mechanical robustness and improved sodium-ion conductivity. Energy Storage Materials, 2019, 21, 85-96.	18.0	43
63	Rational Design of a Multifunctional Binder for High-Capacity Silicon-Based Anodes. ACS Energy Letters, 2019, 4, 1171-1180.	17.4	108
64	Understanding the Low-Voltage Hysteresis of Anionic Redox in Na <sub>2</sub> Mn <sub>3</sub> O <sub>7</sub> . Chemistry of Materials, 2019, 31, 3756-3765.	6.7	112
65	Selenium-sulfur (SeS) fast charging cathode for sodium and lithium metal batteries. Energy Storage Materials, 2019, 20, 71-79.	18.0	50
66	Probing lithiation and delithiation of thick sintered lithium-ion battery electrodes with neutron imaging. Journal of Power Sources, 2019, 419, 127-136.	7.8	46
67	Ion transport and association study of glyme-based electrolytes with lithium and sodium salts. Electrochimica Acta, 2019, 304, 239-245.	5.2	33
68	Structural and Electrochemical Characterization of Thin Film Li2MoO3 Electrodes. Journal of the Electrochemical Society, 2019, 166, A1015-A1021.	2.9	2
69	Probing Electrolyte Solvents at Solid/Liquid Interface Using Gap-Mode Surface-Enhanced Raman Spectroscopy. Journal of the Electrochemical Society, 2019, 166, A178-A187.	2.9	28
70	Effect of Binder Architecture on the Performance of Silicon/Graphite Composite Anodes for Lithium Ion Batteries. ACS Applied Materials & Interfaces, 2018, 10, 3470-3478.	8.0	77
71	Facile and scalable fabrication of polymer-ceramic composite electrolyte with high ceramic loadings. Journal of Power Sources, 2018, 390, 153-164.	7.8	68
72	Frontiers of solid-state batteries. MRS Bulletin, 2018, 43, 740-745.	3.5	35

#	Article	IF	CITATIONS
73	Electrolyte Solvation Structure at Solid–Liquid Interface Probed by Nanogap Surface-Enhanced Raman Spectroscopy. ACS Nano, 2018, 12, 10159-10170.	14.6	70
74	Chemical Evolution in Silicon–Graphite Composite Anodes Investigated by Vibrational Spectroscopy. ACS Applied Materials & Interfaces, 2018, 10, 18641-18649.	8.0	50
75	Synthesis and Electrochemical and Structural Investigations of Oxidatively Stable Li <sub>2</sub> MoO <sub>3</sub> and <i>x</i> Li <sub>2</sub> MoO <sub>3</sub> ·(1 –) Tj ETQq1 1 0.7843	146rgBT / (	Dv <b>ed</b> ock 10
76	Nanostructured Silicon–Carbon 3D Electrode Architectures for High-Performance Lithium-Ion Batteries. ACS Omega, 2018, 3, 9598-9606.	3.5	23
77	Mechanically Robust, Sodium-Ion Conducting Membranes for Nonaqueous Redox Flow Batteries. ACS Energy Letters, 2018, 3, 1640-1647.	17.4	22
78	A comparative study on the oxidation of two-dimensional Ti <sub>3</sub> C <sub>2</sub> MXene structures in different environments. Journal of Materials Chemistry A, 2018, 6, 12733-12743.	10.3	193
79	High Areal Capacity Si/LiCoO 2 Batteries from Electrospun Composite Fiber Mats. ChemSusChem, 2017, 10, 1823-1831.	6.8	22
80	Structural Transformations in High-Capacity Li <sub>2</sub> Cu <sub>0.5</sub> Ni <sub>0.5</sub> O <sub>2</sub> Cathodes. Chemistry of Materials, 2017, 29, 2997-3005.	6.7	21
81	Impact of air exposure and surface chemistry on Li–Li <sub>7</sub> La <sub>3</sub> Zr <sub>2</sub> O <sub>12</sub> interfacial resistance. Journal of Materials Chemistry A, 2017, 5, 13475-13487.	10.3	300
82	Unrivaled combination of surface area and pore volume in micelle-templated carbon for supercapacitor energy storage. Journal of Materials Chemistry A, 2017, 5, 13511-13525.	10.3	63
83	Electrochemical performance of MXenes as K-ion battery anodes. Chemical Communications, 2017, 53, 6883-6886.	4.1	157
84	Self-Assembly of Large Gold Nanoparticles for Surface-Enhanced Raman Spectroscopy. ACS Applied Materials & Interfaces, 2017, 9, 13457-13470.	8.0	104
85	Stable Electrolyte for High Voltage Electrochemical Double-Layer Capacitors. Journal of the Electrochemical Society, 2017, 164, A277-A283.	2.9	25
86	Multimodality of Structural, Electrical, and Gravimetric Responses of Intercalated MXenes to Water. ACS Nano, 2017, 11, 11118-11126.	14.6	183
87	Freeze Tape Cast Thick Mo Doped Li <sub>4</sub> Ti <sub>5</sub> O <sub>12</sub> Electrodes for Lithium-Ion Batteries. Journal of the Electrochemical Society, 2017, 164, A2603-A2610.	2.9	32
88	Crystal Chemistry and Electrochemistry of LixMn1.5Ni0.5O4 Solid Solution Cathode Materials. Chemistry of Materials, 2017, 29, 6818-6828.	6.7	24
89	Engineering Redox Potential of Lithium Clusters for Electrode Material in Lithium-Ion Batteries. Journal of Cluster Science, 2017, 28, 2779-2793.	3.3	13
90	Synthesis and Characterization of 2D Molybdenum Carbide (MXene). Advanced Functional Materials, 2016, 26, 3118-3127.	14.9	945

#	Article	IF	CITATIONS
91	Promotional Effects of In on Non-Oxidative Methane Transformation Over Mo-ZSM-5. Catalysis Letters, 2016, 146, 1903-1909.	2.6	10
92	Probing Multiscale Transport and Inhomogeneity in a Lithium-Ion Pouch Cell Using In Situ Neutron Methods. ACS Energy Letters, 2016, 1, 981-986.	17.4	43
93	Twoâ€Ðimensional Nbâ€Based M <sub>4</sub> C <sub>3</sub> Solid Solutions (MXenes). Journal of the American Ceramic Society, 2016, 99, 660-666.	3.8	234
94	Characterizing the Li–Li7La3Zr2O12 interface stability and kinetics as a function of temperature and current density. Journal of Power Sources, 2016, 302, 135-139.	7.8	446
95	A cellulose nanocrystal-based composite electrolyte with superior dimensional stability for alkaline fuel cell membranes. Journal of Materials Chemistry A, 2015, 3, 13350-13356.	10.3	51
96	In Situ Localized Surface Plasmon Resonance (LSPR) Spectroscopy to Investigate Kinetics of Chemical Bath Deposition of CdS Thin Films. Journal of Physical Chemistry C, 2015, 119, 5033-5039.	3.1	22
97	Controlled Formation of Mixed Nanoscale Domains of High Capacity Fe <sub>2</sub> O <sub>3</sub> –FeF <sub>3</sub> Conversion Compounds by Direct Fluorination. ACS Nano, 2015, 9, 2530-2539.	14.6	51
98	Correlating Local Structure with Electrochemical Activity in Li <sub>2</sub> MnO <sub>3</sub> . Journal of Physical Chemistry C, 2015, 119, 18022-18029.	3.1	26
99	Three-Dimensionally Mesostructured Fe <sub>2</sub> O <sub>3</sub> Electrodes with Good Rate Performance and Reduced Voltage Hysteresis. Chemistry of Materials, 2015, 27, 2803-2811.	6.7	74
100	Large-scale delamination of multi-layers transition metal carbides and carbonitrides "MXenes― Dalton Transactions, 2015, 44, 9353-9358.	3.3	662
101	Synthesis, Structure, and Electrochemical Performance of High Capacity Li <sub>2</sub> Cu <sub>0.5</sub> Ni <sub>0.5</sub> O <sub>2</sub> Cathodes. Chemistry of Materials, 2015, 27, 6746-6754.	6.7	31
102	High-capacity electrode materials for electrochemical energy storage: Role of nanoscale effects. Pramana - Journal of Physics, 2015, 84, 1073-1086.	1.8	9
103	Facet-Dependent Disorder in Pristine High-Voltage Lithium–Manganese-Rich Cathode Material. ACS Nano, 2014, 8, 12710-12716.	14.6	71
104	Thermophysical properties of LiFePO4 cathodes with carbonized pitch coatings and organic binders: Experiments and first-principles modeling. Journal of Power Sources, 2014, 251, 8-13.	7.8	30
105	Effect of interface modifications on voltage fade in 0.5Li2MnO3·0.5LiNi0.375Mn0.375Co0.25O2 cathode materials. Journal of Power Sources, 2014, 249, 509-514.	7.8	89
106	Electrode architectures for high capacity multivalent conversion compounds: iron (ii and iii) fluoride. RSC Advances, 2014, 4, 6730.	3.6	39
107	Monolithic Composite Electrodes Comprising Silicon Nanoparticles Embedded in Ligninâ€derived Carbon Fibers for Lithiumâ€lon Batteries. Energy Technology, 2014, 2, 773-777.	3.8	22
108	Artificial Solid Electrolyte Interphase To Address the Electrochemical Degradation of Silicon Electrodes. ACS Applied Materials & amp; Interfaces, 2014, 6, 10083-10088.	8.0	141

#	Article	IF	CITATIONS
109	Role of Surface Functionality in the Electrochemical Performance of Silicon Nanowire Anodes for Rechargeable Lithium Batteries. ACS Applied Materials & Interfaces, 2014, 6, 7607-7614.	8.0	30
110	Nanoscale Morphological and Chemical Changes of High Voltage Lithium–Manganese Rich NMC Composite Cathodes with Cycling. Nano Letters, 2014, 14, 4334-4341.	9.1	163
111	An Artificial Solid Electrolyte Interphase Enables the Use of a LiNi <sub>0.5</sub> Mn <sub>1.5</sub> O <sub>4</sub> 5 V Cathode with Conventional Electrolytes. Advanced Energy Materials, 2013, 3, 1275-1278.	19.5	75
112	Formation of Iron Oxyfluoride Phase on the Surface of Nano-Fe3O4 Conversion Compound for Electrochemical Energy Storage. Journal of Physical Chemistry Letters, 2013, 4, 3798-3805.	4.6	28
113	Solid electrolyte coated high voltage layered–layered lithium-rich composite cathode: Li1.2Mn0.525Ni0.175Co0.1O2. Journal of Materials Chemistry A, 2013, 1, 5587.	10.3	137
114	A Perspective on Coatings to Stabilize High-Voltage Cathodes: LiMn <sub>1.5</sub> Ni <sub>0.5</sub> O <sub>4</sub> with Sub-Nanometer Lipon Cycled with LiPF <sub>6</sub> Electrolyte. Journal of the Electrochemical Society, 2013, 160, A3113-A3125.	2.9	51
115	Electrochemical Stability of Carbon Fibers Compared to Aluminum as Current Collectors for Lithium-Ion Batteries. Journal of the Electrochemical Society, 2012, 159, A1652-A1658.	2.9	48
116	Conductive surface modification of LiFePO4 with nitrogen-doped carbon layers for lithium-ion batteries. Journal of Materials Chemistry, 2012, 22, 4611.	6.7	76
117	Surface studies of high voltage lithium rich composition: Li1.2Mn0.525Ni0.175Co0.1O2. Journal of Power Sources, 2012, 216, 179-186.	7.8	131
118	Anomalous Discharge Product Distribution in Lithium-Air Cathodes. Journal of Physical Chemistry C, 2012, 116, 8401-8408.	3.1	79
119	Influence of Lithium Salts on the Discharge Chemistry of Li–Air Cells. Journal of Physical Chemistry Letters, 2012, 3, 1242-1247.	4.6	123
120	Atomically localized plasmon enhancement in monolayer graphene. Nature Nanotechnology, 2012, 7, 161-165.	31.5	196
121	Electrochemical and rate performance study of high-voltage lithium-rich composition: Li1.2Mn0.525Ni0.175Co0.1O2. Journal of Power Sources, 2012, 199, 220-226.	7.8	210
122	Spectroscopic Characterization of Solid Discharge Products in Li–Air Cells with Aprotic Carbonate Electrolytes. Journal of Physical Chemistry C, 2011, 115, 14325-14333.	3.1	114
123	Advanced Lithium Battery Cathodes Using Dispersed Carbon Fibers as the Current Collector. Journal of the Electrochemical Society, 2011, 158, A1060.	2.9	59
124	Direct synthesis of nanostructured V2O5 films using solution plasma spray approach for lithium battery applications. Journal of Power Sources, 2011, 196, 10704-10711.	7.8	29
125	Local Stateâ€ofâ€Charge Mapping of Lithiumâ€ŀon Battery Electrodes. Advanced Functional Materials, 2011, 21, 3282-3290.	14.9	102
126	High voltage stability of LiCoO2 particles with a nano-scale Lipon coating. Electrochimica Acta, 2011, 56, 6573-6580.	5.2	91

#	Article	IF	CITATIONS
127	In situ Raman microscopy during discharge of a high capacity silicon–carbon composite Li-ion battery negative electrode. Electrochemistry Communications, 2009, 11, 235-237.	4.7	71
128	Multiangle Depolarized Dynamic Light Scattering of Short Functionalized Single-Walled Carbon Nanotubes. Journal of Physical Chemistry C, 2009, 113, 7129-7133.	3.1	59
129	Thermal Conductivity of Single-Wall Carbon Nanotube Dispersions:  Role of Interfacial Effects. Journal of Physical Chemistry C, 2008, 112, 654-658.	3.1	88
130	Light Amplification in the Single-Exciton Regime Using Excitonâ^'Exciton Repulsion in Type-II Nanocrystal Quantum Dots. Journal of Physical Chemistry C, 2007, 111, 15382-15390.	3.1	84
131	Single-exciton optical gain in semiconductor nanocrystals. Nature, 2007, 447, 441-446.	27.8	894
132	Type-II Core/Shell CdS/ZnSe Nanocrystals:  Synthesis, Electronic Structures, and Spectroscopic Properties. Journal of the American Chemical Society, 2007, 129, 11708-11719.	13.7	402
133	Effect of the Thiolâ^'Thiolate Equilibrium on the Photophysical Properties of Aqueous CdSe/ZnS Nanocrystal Quantum Dots. Journal of the American Chemical Society, 2005, 127, 10126-10127.	13.7	224
134	Light Amplification Using Inverted Core/Shell Nanocrystals:Â Towards Lasing in the Single-Exciton Regime. Journal of Physical Chemistry B, 2004, 108, 10625-10630.	2.6	165
135	Challenges for and Pathways toward Li-Metal-Based All-Solid-State Batteries. ACS Energy Letters, 0, , 1399-1404.	17.4	228